Transport Processes in Reacting Hydrothermal Flames with Applications to Military Waste Destruction in Supercritical Water and Geotechnical Rock Excavation

Department of Chemical Engineering
Massachusetts Institute of Technology
77 Massachusetts Avenue
Room 66-454
Cambridge, MA 02139

Telephone: 617-253-7090
Fax: 617-258-5042
Email: testerel@mit.edu

Authors: J.W. Tester
C. Augustine

Final Report to U.S. Army Research Office
For the Period September 15, 2005 – March 14, 2009

P.O. Box 12211
Research Triangle Park, NC 27709-2211

Report Documentation Page

Form Approved
OMB No. 0704-0188

1. REPORT DATE	2. REPORT TYPE	3. DATES COVERED
2009		**00-00-2009 to 00-00-2009**

4. TITLE AND SUBTITLE	5a. CONTRACT NUMBER
Transport Processes in Reacting Hydrothermal Flames with Applications to Military Waste Destruction in Supercritical Water and Geotechnical Rock Excavation	**W911NF-05-1-0522**
	5b. GRANT NUMBER
	5c. PROGRAM ELEMENT NUMBER
6. AUTHOR(S)	5d. PROJECT NUMBER
	5e. TASK NUMBER
	5f. WORK UNIT NUMBER
7. PERFORMING ORGANIZATION NAME(S) AND ADDRESS(ES) **Department of Chemical Engineering,Massachusetts Institute of Technology,77 Massachusetts Avenue, Room 66-454,Cambridge,MA,02139-4307**	8. PERFORMING ORGANIZATION REPORT NUMBER **; 46955-CH.1**
9. SPONSORING/MONITORING AGENCY NAME(S) AND ADDRESS(ES) **U.S. Army Research Office, P.O. Box 12211, Research Triangle Park, NC, 27709-2211**	10. SPONSOR/MONITOR'S ACRONYM(S)
	11. SPONSOR/MONITOR'S REPORT NUMBER(S) **46955-CH.1**

12. DISTRIBUTION/AVAILABILITY STATEMENT
Approved for public release; distribution unlimited

13. SUPPLEMENTARY NOTES

14. ABSTRACT

15. SUBJECT TERMS

16. SECURITY CLASSIFICATION OF:			17. LIMITATION OF ABSTRACT	18. NUMBER OF PAGES	19a. NAME OF RESPONSIBLE PERSON
a. REPORT **unclassified**	b. ABSTRACT **unclassified**	c. THIS PAGE **unclassified**	**Same as Report (SAR)**	**16**	

1. Overview

A hydrothermal flame is a flame that exists in a supercritical aqueous medium and is characterized by steep temperature and density gradients. The overall objective of our project was to increase understanding of heat, mass, and momentum transport processes within hydrothermal flames. Specifically, we planned to study hydrothermal flame characteristics such as flame temperature and stability, and to develop a method for modeling heat and mass transport processes in the hydrothermal flame and supercritical water environments based on experimental observations. With this knowledge, hydrothermal flames can be tailored to the task of destroying aqueous wastes such as chemical and biological warfare agents or municipal sludges, or used to perform thermal spallation and/or fusion of rock surfaces in a deep-borehole environment for rock drilling and excavation.

An autoclave reaction system was designed and constructed to create flame jets in water using both methanol and hydrogen as fuel at a pressure of 250 bar. The temperatures of these flames were measured, and attempts were made to use the flames to spall small rock samples. The experimental system was modified to study the centerline temperature decay of supercritical water jets injected at temperatures up to 525 ^{o}C into ambient temperature water. A device for measuring the heat flux from these jets was designed, constructed, and used to determine the heat transfer coefficients of the jets impinging against a flat surface. Together, these studies indicate that the necessary temperatures and heat fluxes required to induce thermal spallation in rocks can be achieved in a deep borehole. A detailed account of the experiments and results summarized below is available in Thesis Dissertation "Hydrothermal Spallation Drilling and Advanced Energy Conversion for Engineered Geothermal Systems" by Chad Augustine, which will be available online at http://dspace.mit.edu/ in the near future.

2. Wall-Cooled Hydrothermal Burner Reactor System

The Wall-Cooled Hydrothermal Burner (WCHB) reactor system is used to create diffusion flames in a high pressure, aqueous environment. Figure 1 provides a flowsheet of the entire WCHB reactor system, while a detailed schematic of the WCHB reactor itself is shown in Figure 2. The WCHB reactor has three co-axial feed streams: the fuel feed, which travels down the center tube, the oxygen feed, which is in the annulus surrounding and adjacent to the fuel feed and combines with the fuel in the combustion chamber to initiate combustion, and the cooling water feed, which is in the outermost annulus and forms a sub-critical temperature barrier that protects the reactor walls from the flame. Either methanol or hydrogen can be used as a fuel in the current configuration, although the use of other fuels is possible. The WCHB reactor also has two sapphire windows for optical observations.

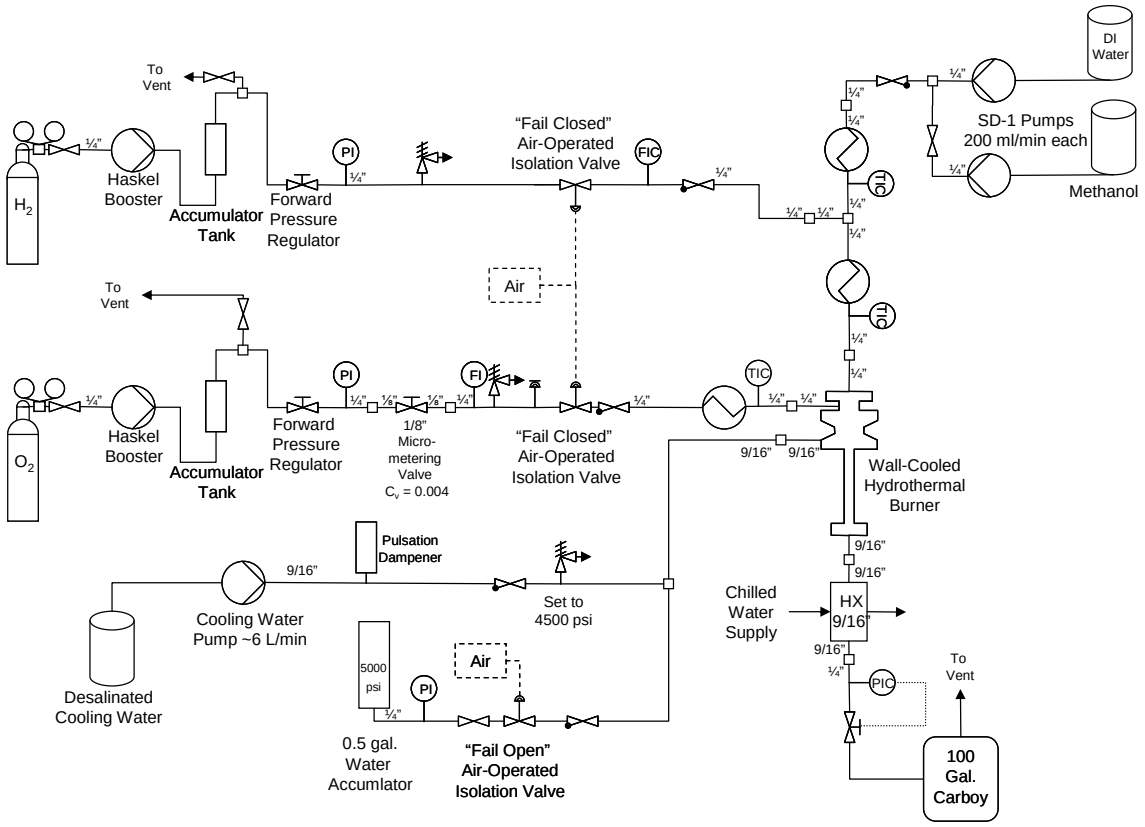

Figure 1. Schematic of WCHB reaction system.

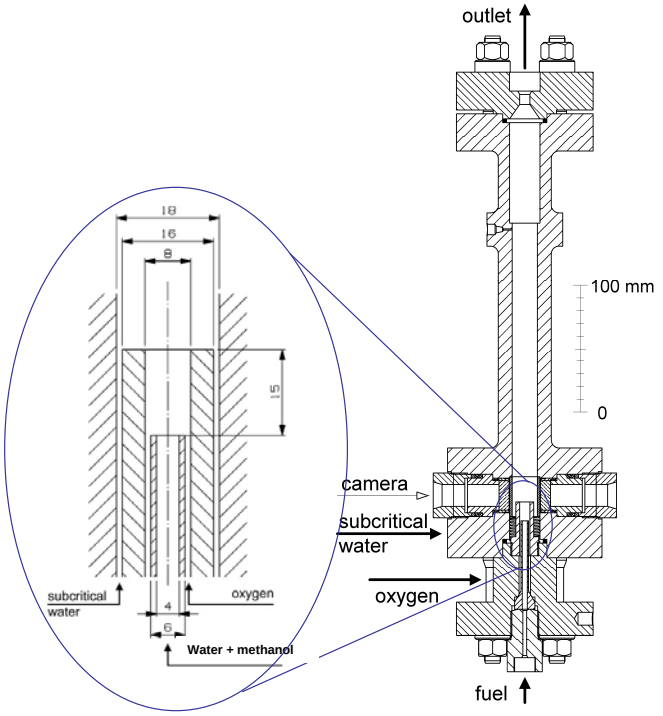

Figure 2. Schematic of WCHB reactor with close-up of burner nozzle design.

Data collection from the WCHB reactor as it was originally designed is limited by the number of ports available in the head of the vessel for instrumentation. Moreover, once instrumentation is installed via these ports, it is fixed in position, severely limiting the regions of the vessel that can be measured. A means of measuring or sampling a range of positions in the WCHB reactor space during operation was desired. Therefore, an apparatus capable of positioning a probe dynamically in the WCHB reactor during the course of an experiment while still maintaining system pressure was designed and constructed. The apparatus was named the movable probe assembly.

The movable probe assembly consists of a piston mounted on a ¼" (6.35 mm) OD tube mounted inside a special cylindrical housing (Figure 3). The movable probe assembly is mounted at the WCHB reactor outlet, while the tube extends the length of the vessel to the combustion chamber. The piston has two Viton O-rings that center it and separate the process fluid from the hydraulic fluid used to move the piston. During operation, high pressure hydraulic fluid is injected or removed to move the piston, traversing the probe tip along the axis of the reaction vessel. The piston has about 3.25" (80 mm) of travel inside the housing. Another Viton O-ring at the exit of the cylindrical housing forms a high-pressure seal while allowing the rod to slide into and out of the assembly. The cylindrical housing is connected to a tee with a High Pressure Equipment Company (HIP) adapter fitting. A 9/16" (14.3 mm) OD nipple connects the tee to the reactor outlet port of the WCHB-1 reactor to seal and maintain the reactor system pressure. The cylindrical housing and piston were fabricated by the MIT Central machine shop. SS316 was used as the material of construction. The piston was welded to the ¼" (6.4 mm) HP tubing.

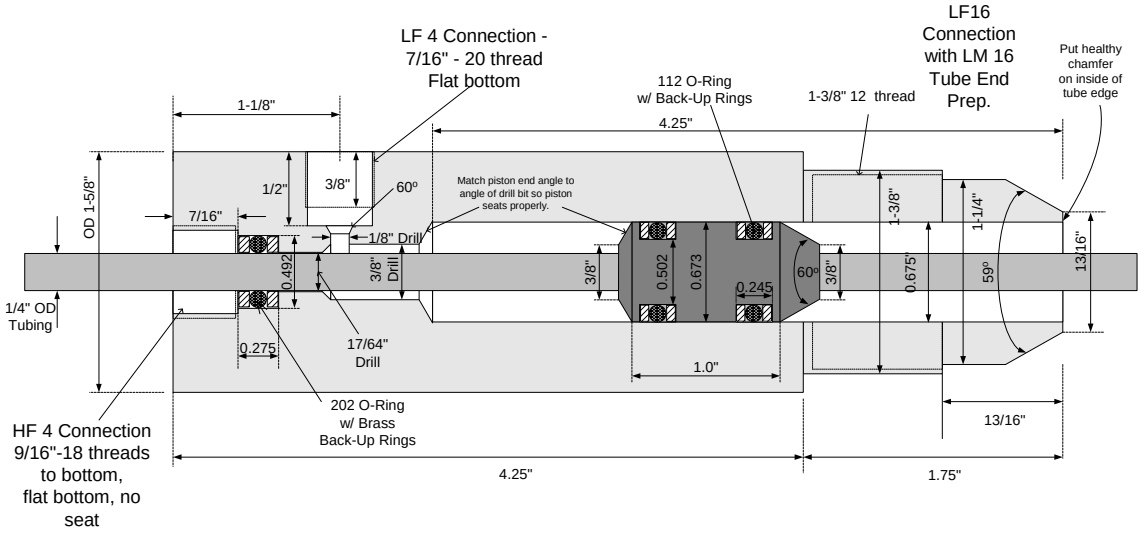

Figure 3. Technical drawing of movable probe assembly cylindrical housing and tube-mounted piston, as assembled. All dimenstions are in inches (″). Connection types (ex. – HF4) refer to details for HIP pressure connections (High Pressure Equipment Company, 2009).

The movable probe assembly enables several possible experiments to be carried out. The rod is hollow, so that a thermocouple can be passed through the rod into the reactor. The probe can then be moved through a hydrothermal flame during operation so that

temperature as a function of axial position can be determined. A heat flux meter can also be mounted at the end of the probe to determine heat flux from the hydrothermal flame to a flat surface as a function of stand-off distance. Finally, a rock sample can be mounted on the probe to determine if hydrothermal flames are capable of spalling rock at conditions simulating a deep borehole environment.

3. Hydrothermal flame experiments

Experiments studying the extinction behavior of hydrothermal flame using mixtures of both water and methanol and water and hydrogen as fuel were performed. Table 1 shows the operating conditions at the point of flame ignition for all experiments performed using methanol as a fuel. The point of flame ignition was determined by a sudden increase in temperatures measured by the thermocouples positioned above the combustion chamber exit and at the reactor outlet. Most of the experiments used a fuel mixture of 25 mass% methanol because it was easily ignited but did not result in excessively high flame temperatures. The observed ignition temperatures for 25 mass% fuel span a range of about 50 ^{o}C.

Table 1. Operating conditions at point of autoignition for hydrothermal flames using methanol as fuel.

Date	Mass % Methanol	Fuel Mixture			O_2	CW	T_{fuel}	T_{O2}
		Methanol	Water	Total				
	(%)	(g/s)	(g/s)	(g/s)	(g/s)	(g/s)	(^{o}C)	(^{o}C)
6/19/06[1]	25	0.200	0.60	0.8	0.45	3.17	538	413
8/21/06	25	0.375	1.13	1.5	0.84	35	506	454
11/6/06	25	0.313	0.94	1.25	0.70	45	547	409
12/12/06[2]	21.2-23.2	0.30-0.31	1.00-1.17	1.48	0.56[3]	40	547	439
7/30/07	25	0.375	1.13	1.5	0.84	40	497	428
7/30/07	25	0.375	1.13	1.5	0.84	30	507	440
9/7/07	25	0.375	1.13	1.5	0.90	40	532	417
9/17/07	28.1	0.367	0.94	1.31	0.65[3]	35	545	448
9/18/07	35.8	0.419	0.75	1.17	0.84[3]	35	539	423

[1]First successful ignition, performed using SD-1 pump to provide cooling water.
[2]Ignition occurred during increase in methanol flow rate, actual methanol flowrate unknown.
[3]Oxygen flow rates not 150% stoichiometric at time of ignition.

Table 2 lists the observed operating conditions at the point of extinction for the methanol flame experiments in which flame extinction was either not intentional or the result of some experimental error. The last recorded methanol flame extinction on July 30, 2007 occurred at a fuel mixture temperature of 85 ^{o}C. A lower fuel extinction temperature may have been possible, but the WCHB system ran out of methanol fuel and ended the experiment prematurely. The results are comparable to those of previous researchers and show that methanol hydrothermal flames can achieve stable combustion even when the temperature of the incoming feed streams are decreased well below their autoignition temperatures.

Table 2. Operating conditions at point of extinction for hydrothermal flames with methanol fuel.

Date	Mass % Methanol	Fuel Mixture			O_2	CW	T_{fuel}	T_{O2}
		Methanol	Water	Total				
	(%)	(g/s)	(g/s)	(g/s)	(g/s)	(g/s)	(^oC)	(^oC)
8/21/06[1]	25	0.375	1.13	1.5	0.84	42.5	258	196
11/6/06	20	0.313	0.94	1.25	0.45	45	428	260
7/30/07	25	0.375	1.13	1.5	0.84	45	85	360

[1]Extinction believed to be caused by air bubble in methanol feed line.

Following the successful demonstration of creating hydrothermal flames using methanol as a fuel, the feasibility of using hydrogen as a fuel was explored. These are the first known experiments performed using hydrogen as a fuel in hydrothermal flame experiments. Ignition behavior was not explored because numerous attempts to ignite a flame using hydrogen as fuel were unsuccessful, except for one instance which could not be duplicated. Therefore, a system was developed in which the flames were ignited using a methanol fuel mixture, and then the fuel source was slowly switched over from methanol to hydrogen. The conditions at the point of extinction for 3 successful experiments are shown in Table 3. The fuel inlet temperature at the point of extinction is very similar for the three experiments, especially for the cases where 4 wt% H_2 was used as fuel. This indicates that the experiments are both repeatable and representative of true extinction behavior. The flame is quickly quenched, even only a short distance above the nozzle exit. Unlike hydrothermal flames made with methanol, the temperature of the feed streams for flames made with hydrogen could not be decreased significantly below the critical temperature of water. It is believed that de-mixing of the water-hydrogen feed below the critical temperature of water leads to flame instability. Further experiments were not carried out due to the desire to use the reactor system to perform different experiments, described below.

Table 3. Experimental conditions for hydrogen hydrothermal flame experiments at point of extinction.

Experiment Description	Fuel Mixture		O_2	Cooling Water	O_2 inlet Temp	Fuel inlet temp	Temp ~1 cm above nozzle
	H_2	Water					
	g/s	g/s	g/s	g/s	(^oC)	(^oC)	(^oC)
4 wt% H2 @ 1.25 g/s	0.050	1.2	0.60	35	321	**322**	265
4 wt% H2 @ 1.5 g/s	0.060	1.44	0.71	35	301	**317**	285
3 wt% H2 @ 1.25 g/s	0.038	1.21	0.45	35	360	**335**	253

4. Flame jet thermal spallation experiments

4.1 Stagnation temperature measurements

The stagnation temperature refers to the temperature at the point of jet impingement on a surface, and will vary with stand-off distance due to entrainment of the surrounding cooling water. Stagnation temperatures for flame jets impinging against a flat surface were measured using a thermocouple passed through a Macor ceramic block mounted in the movable probe reactor. A hydrothermal flame was ignited in the WCHB system using methanol as fuel. Table 4 shows the range of methanol fuel concentrations and flow rates studied. Once the flame was stabilized at the desired operating conditions, the Macor block was moved to a stand-off distance of 15 mm, and data collection began. The stand-off distance between the Macor block face and the jet nozzle exit could be varied during the course of the experiment in increments as small as 0.01 mm using the movable probe assembly. The stagnation temperature of the impinging jet flame was measured in 1 to 2 mm intervals along the centerline axis of the jet. Close to the jet nozzle exit, where temperatures increased rapidly as the stand-off distance decreased, the spacing between measurements was decreased to 0.25 to 0.50 mm intervals. At each stand-off distance, temperatures were recorded at a rate of once per second over a 1-minute period. For the 15 mass% methanol fuel mixture flames, the Macor block was lowered to within 1.5 mm of the jet nozzle exit. For the 20 mass% case, a stand-off distance of 3.75 mm was used due to the higher flame temperatures to avoid damaging the Macor block and thermocouple.

Table 4. Flow rates and operating conditions for methanol hydrothermal flames used in stagnation temperature study.

Mass % Methanol	Fuel Mixture			O_2	CW	T_{fuel}	T_{O2}
	Methanol	Water	Total				
(%)	(g/s)	(g/s)	(g/s)	(g/s)	(g/s)	(^oC)	(^oC)
15	0.188	1.06	1.25	0.42	50	495	390
15	0.225	1.23	1.50	0.50	50	500	395
20	0.25	1.00	1.25	0.56	50	500	395

The average stagnation temperature with a 95% confidence interval (CI) for the hydrothermal flames produced are shown in Figure 4. The data show that the flame jet is rapidly quenched as it entrains the surrounding cooling water, as had been inferred from the thermocouple positioned above the combustion chamber exit in the earlier study. For each of the flame jets, there are two distinct regions, separated by the critical temperature of water. In the far-field region, when the stagnation temperature is below the critical temperature of water, the rate of stagnation temperature decay as a function of stand-off distance is relatively low. In the near-field region close to the jet nozzle exit, when the stagnation temperature is above the critical temperature of water, the stagnation temperature decay is much more rapid. Close to the jet exit, the stagnation temperature appears to level off to a constant value for the 15 mass% methanol cases, indicating that the center of the Macor block is likely in the core region of the jet, where entrainment of

the surrounding fluid is minimal. The flame temperature of the 20 mass% methanol fuel was too high to attempt to use the Macor block in the core region.

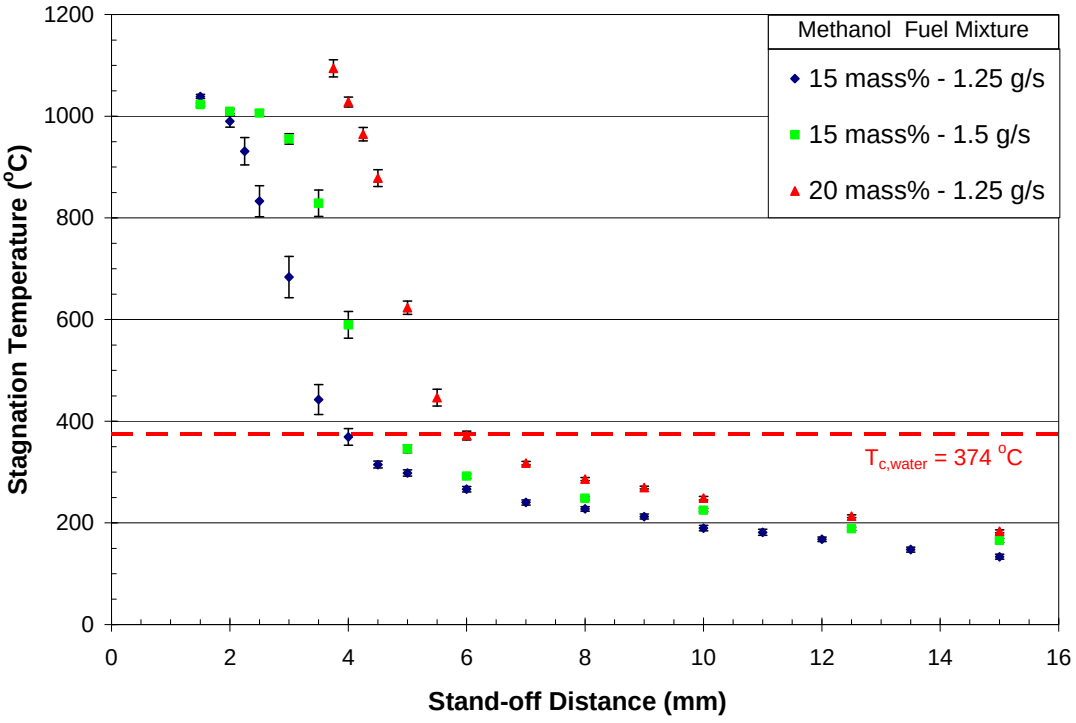

Figure 4. Average stagnation temperature (95% CI) as a function of stand-off distance for methanol hydrothermal flames.

4.2 Rock spallation experiments

An attempt was made to spall rocks using hydrothermal flames in the WCHB. For the rock spallation experiment, a cylindrical sample (17.6 mm OD x 25 mm length) of Sioux quartzite was attached to a nut using epoxy and mounted on the end of the rock carrier and installed in the WCHB reactor. Sioux quartzite was chosen because previous studies had shown it to spall readily at low surface temperature (~350 °C) over a wide range of heat fluxes. A hydrothermal flame was ignited using methanol as fuel. As in the stagnation temperature experiments, several attempts were needed to achieve ignition. Once ignited, the operating conditions were adjusted to same conditions used for the 1.5 g/s flow rate of 15 mass% methanol fuel mixture case in Table 4. Once the operating conditions had stabilized, the rock was lowered into the flame jet. Based on stagnation temperature measurement, the rock surface was positioned at a stand-off distance of 1.5 mm, which should result in a jet with a stagnation temperature of ~1025 °C impinging on the rock surface. The rock was left at this position for 5 minutes before it was withdrawn from the flame jet. The flame was extinguished, the WCHB system shut down, and the Sioux Quartzite rock sample was removed for inspection.

Based on examination of the Sioux quartzite rock surface, it appears that spallation did occur initially, but quickly stopped, resulting in a very shallow hole, about 10 mm in diameter and 1 to 2 mm deep (Figure 5). Because of the relatively small rock sample sizes used, too large a portion of the surface of the rock is heated up and expanded, such

that sufficient confining stress could not build up to maintain spallation. This is supported by the presence of several cracks that emanated radially from the center of the rock sample and over its entire length.

Figure 5. Sioux quartzite successfully spalled using 15 mass% methanol fuel flame jet.

An attempt was made to spall a sample of Westerly granite. Once again, difficulties were encountered while trying to ignite the hydrothermal flame. In one experiment, the flow rate of water was reduced to increase the methanol fuel mixture concentration entering the reactor. At some point, the fuel ignited. An intense white flame was observed through the sapphire view ports. Temperatures of 1510 ^{o}C and 1260 ^{o}C were recorded by the fuel mixture and oxygen inlet thermocouples, respectively. The intense flame burned for only several seconds. The flame was shortly followed by a large leak from the reactor head. The experiment was halted and the WCHB system immediately shut down. The reactor was disassembled and inspected for damage. The fuel nozzle was severely damaged – only its base remained; the tubing had either burned away, which would explain the intense white flame, or had been melted. The fuel mixture and oxygen thermocouples were also damaged. The cooling water flow was sufficient to protect the reactor walls and oxygen nozzle from damage as it had been designed. This incident, along with the general difficulties encountered in igniting flames reinforce a concern that the WCHB reactor is too small to accommodate sufficiently large rock samples to permit continuous, steady-state spallation.

5. Supercritical Jets in Subcritical Co-Flow

After the observations of the rapid quenching of the hydrothermal flame jet in subcritical water, a study was conducted to characterize the behavior of free turbulent jets at supercritical temperatures in subcritical temperature co-flow. It was not necessary to create flame jets to study this behavior – the WCHB reactor system is capable of producing jets of water at temperatures up to 525 ^{o}C, well above the critical temperature of water (374 ^{o}C). With proper scaling of the experimental variables, these supercritical jets should provide insight into the behavior of low density, supercritical temperature jets in a high density, subcritical temperature environment without having to overcome the

documented difficulty in creating, maintaining, and studying flame jets in water at high pressures. Ideally, it would be possible to fully characterize the jets by measuring both the temperature and velocity profiles as a function of axial and radial position. However, the experimental setup of the WCHB reactor system only permitted the reliable measurement of the centerline axial temperature profile. Therefore, the centerline axial temperature behavior of jets of water at both supercritical and subcritical temperatures in co-flowing, ambient temperature (~25 ^{o}C) cooling water was studied.

The WCHB and movable probe assembly with a single thermocouple inserted along the centerline axis, capable of accurately measuring the centerline jet temperature as a function of axial position, was used to determine the behavior of sub- and supercritical jets in a subcritical co-flow. Jet nozzle exit temperatures ranging from 300 to 525 ^{o}C, corresponding to initial density ratios ranging from 1.35 to 12.1, were studied. The jet was divided into two regions: the far-field region and the jet development region. In the far-field, the flow in the jet was characterized as a free turbulent jet, with negligible effects from buoyancy or the co-flowing cooling water. Conditions under which recirculation zones affected jet behavior were identified and removed from experimental consideration. A similarity analysis was applied to the flow. In the far-field, where the density gradient between the jet and ambient fluid was small, the jet behavior was self-similar, so that the axial temperature decay follows conventional jet scaling laws. The axial position of the jet, X_{eff}, was scaled using the Thring-Newby scaling law:

$$X_{eff} = \frac{x}{D_{eff}} = \frac{x}{D_o}\left(\frac{\rho_o}{\rho_a}\right)^{-1/2} \qquad \text{Eq. (1)}$$

while the axial temperature decay, θ, was scaled with respect to the jet nozzle exit temperature and the temperature of the ambient fluid:

$$\theta = \frac{T - T_a}{T_o - T_a} \qquad \text{Eq. (2)}$$

Figure 6 shows that for a non-buoyant axisymmetric turbulent jet, the centerline temperature decay in the self-similar region is found to decay inversely with axial position:

$$\theta^{-1} = c_1 \frac{(x - x_o)}{D_{eff}} = c_1 X'_{eff} \qquad \text{Eq. (3)}$$

where: x_o = jet virtual origin

X'_{eff} = non-dimensional scaled axial position, corrected for virtual origin

c_1 = constant

The Thring-Newby scaling law accurately accounted for the large initial density ratio between the nozzle exit and ambient fluid. However, the slope of the axial decay of the jets varied slightly as a function of the initial density ratio. The variation is most likely attributable to experimental conditions rather than being a characteristic of the axial temperature decay of supercritical jets.

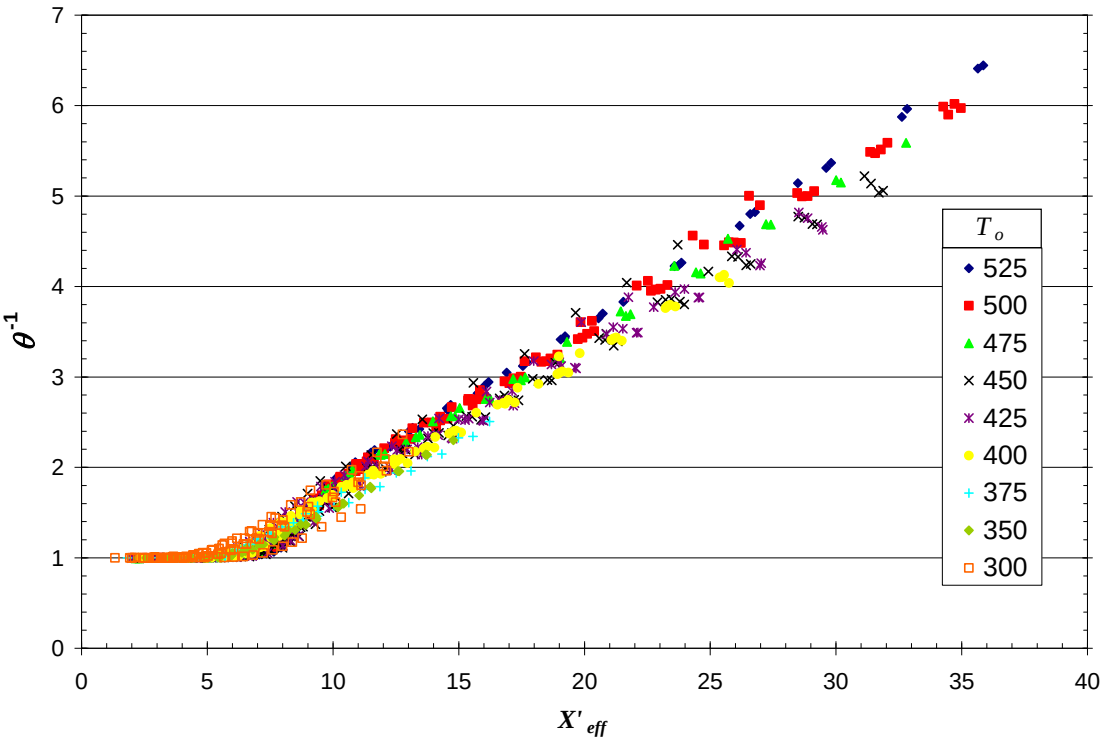

Figure 6. Correlation of centerline temperature as a function of axial position for all experiments over a wide range of nozzle exit temperatures.

In the jet development region, supercritical jets were observed to be quickly quenched to below the critical temperature of water within one or two diameters of the nozzle exist by the ambient fluid. When the Thring-Newby scaling law was applied to the axial length scale, the effective axial distance at which the centerline temperature transitioned from supercritical to subcritical values was roughly the same for all supercritical jet temperatures studied. A model of steam jets injected into a supercooled liquid was used to describe the relationship between the nozzle exit temperature and the depth to which the supercritical temperature penetrated. Although the model predictions were qualitatively correct, the degree to which nozzle exit temperature affected the observed penetration distance of the supercritical jet was much less than that predicted by the model. Jet entrainment coefficients were calculated based on the model results. Values of $0.3 < E_o < 0.7$ were observed. The entrainment coefficient varied strongly with the initial density ratio. The entrainment coefficient results indicate that another factor unaccounted for by the proposed model is likely controlling observed jet behavior in the jet development region. The variations in the slope of the temperature decay laws with initial density ratios in the far-field region supports this observation.

6. Heat Flux from Impinging Jets to a Flat Surface

In addition to jet temperatures, the heat flux from supercritical temperature water jets impinging against a flat surface in a high pressure, subcritical water environment was also studied. The objectives of this study was to design a device that could measure the heat flux from an impinging jet in the deep borehole environment (P = 250 bar, high

temperatures) and to use this device to measure the heat flux from supercritical water jets impinging against a flat surface. The goal of the measurements was to determine whether sufficient heat fluxes can be generated under deep borehole conditions to induce thermal spallation and how the heat flux from the impinging jet varies as a function of stand-off distance.

The heat flux from impinging supercritical temperature jets to a flat surface were successfully measured in the MIT WCHB system using specially designed and constructed heat flux meters (HFM's) capable of functioning in the deep borehole environment simulated in the reaction system. The HFM was designed and constructed in collaboration with Potter Drilling LLC. Although hot water jets used in subsequent experiments with the HFM had a maximum temperature of only 525 ^{o}C, the heat flux meter was designed for eventual use with hydrothermal flame jets at either Potter Drilling LLC or within our research group. A two-dimensional model of heat conduction in the HFM was used to optimize its design. Two HFM's were constructed: one using Naval brass for low heat flux measurements and the other using tellurium copper for high heat flux measurements.

The heat transfer from impinging hot water jets to a flat surface was measured using the same hot water jets studied in Section 5. Results of the heat flux measurements using the Naval brass and tellurium copper HFM's are shown in Figure 7 and Figure 8, respectively. The results are limited to a single jet momentum flux to make the results readable. Maximum heat fluxes of 1.7 MW/m^2 and 4.6 MW/m^2 were measured using the brass and copper HFM's, respectively. Stagnation temperatures as a function of stand-off distance were measured for a range of sub- and supercritical temperature jets in a separate experiment. The measured heat flux was not a static property of the jet and stand-off distance, but depended on the jet stagnation temperature, experimental conditions, and HFM used. Much of the behavior of the measured heat flux as a function of stand-off distance could be explained by the stagnation temperature of the impinging jet. The axial decay profiles of the stagnation temperatures of the impinging jet behaved much like the free jets studied in Section 5 – supercritical jets were quenched quickly after the nozzle exit, and the stagnation temperature decay in the far-field scaled inversely with the stand-off distance. The copper HFM was able to measure much higher heat fluxes than the brass HFM due to its higher thermal conductivity. This allowed it to maintain a lower sensor surface temperature, which increased the temperature driving force for convective heat transfer. Because of the relatively lower thermal conductivity of brass, the brass HFM had a higher sensor surface temperature. In addition to lower measured heat fluxes, small temperature differences between the jet and HFM surface in the far-field region resulted in large errors in the calculated heat transfer coefficient for experiments using the brass HFM.

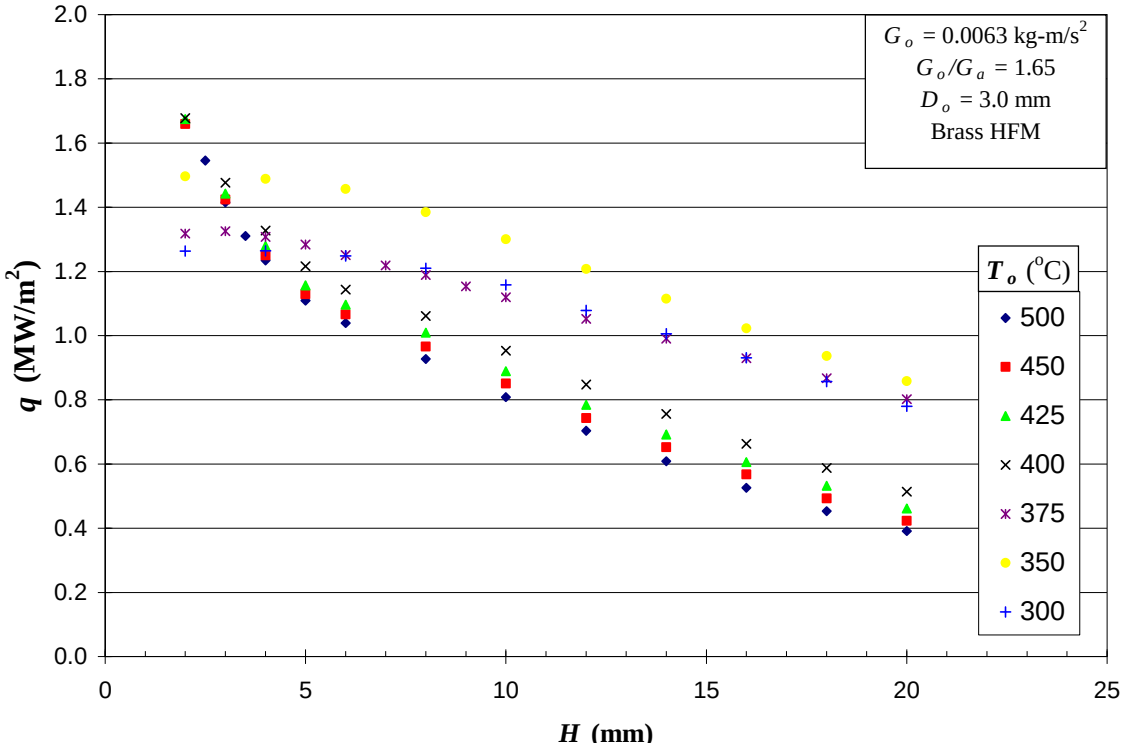

Figure 7. Heat flux from impinging jets to flat surface as a function of stand-off distance for a range of jet nozzle exit temperatures. Heat flux measured using Naval brass HFM.

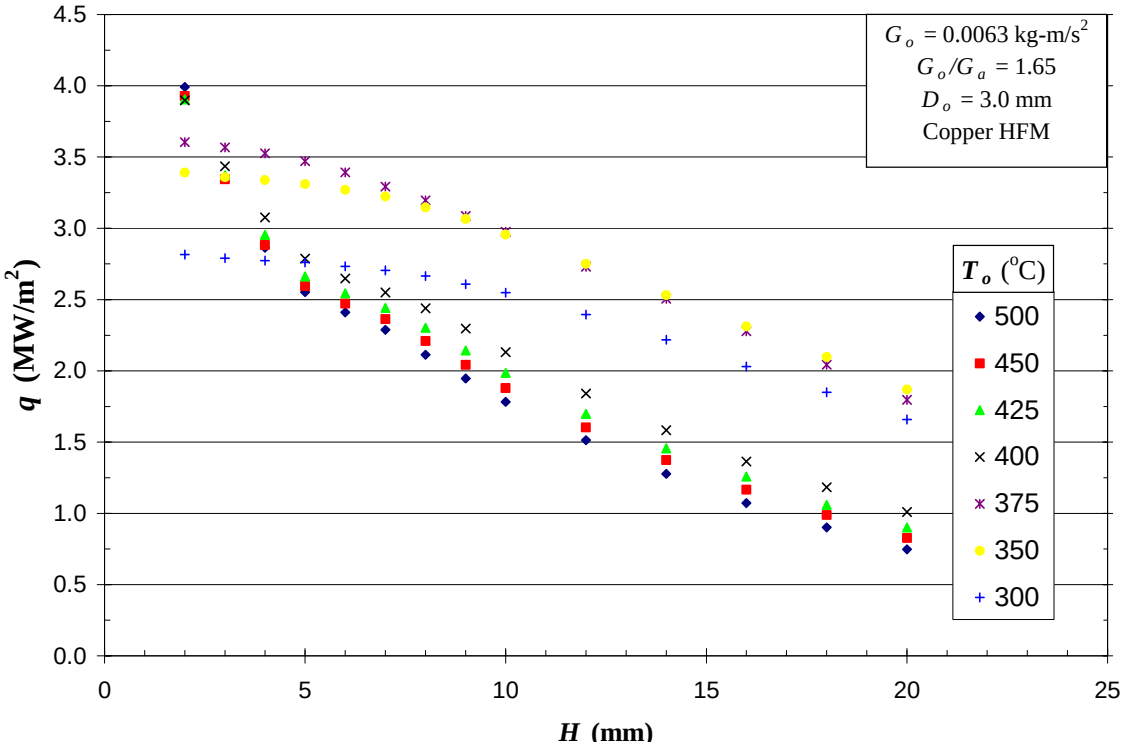

Figure 8. Heat flux from impinging jets to flat surface as a function of stand-off distance for a range of jet nozzle exit temperatures. Heat flux measured using tellurium copper HFM.

The calculated heat transfer coefficient as a function of stand-off distance for experiments performed with the copper HFM are shown in Figure 9 and Figure 10. The copper HFM was able to maintain a large enough temperature difference between the jet and surface that the uncertainty errors of the calculated heat transfer coefficients have 95% confidence intervals of ±10-12% or less. Heat transfer coefficients ranging from 30,000 to 40,000 W/m^2-K were measured at stand-off distances in the far-field region for jets with both sub- and supercritical nozzle exit temperatures. The subcritical temperature jets maintained these high heat transfer coefficients for stand-off distances in the temperature core region of the jet. For supercritical jets, the heat transfer coefficient dropped significantly to values of less than 20,000 W/m^2-K in the area of the jet development region where the stagnation temperature transitions from subcritical to supercritical values. Rapidly increasing stagnation temperatures in this region compensate for the decrease in heat transfer coefficient so that the heat flux from the impinging supercritical temperature jets continually increases as the stand-off distance decreases.

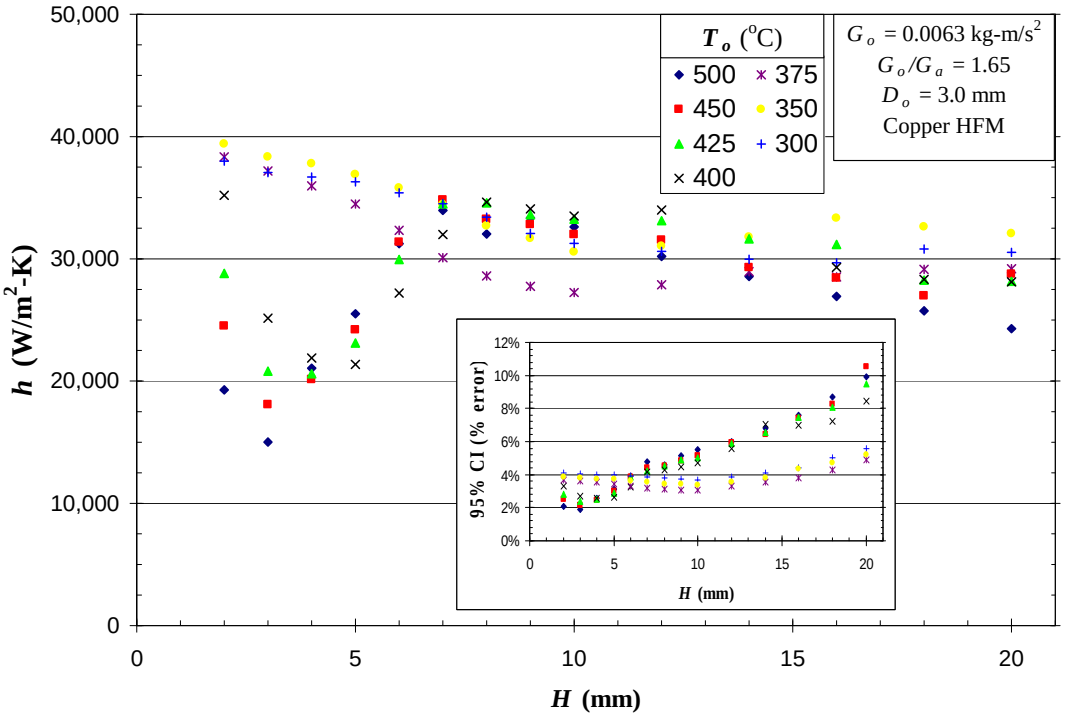

Figure 9. Measured heat flux for jets impinging against a flat surface as a function of stand-off distance for a range of nozzle exit temperatures and jet momentum flux of G_o = 0.0063 kg-m/s^2. (Inset: 95%CI of error measurement as a function of nozzle exit temperature and stand-off distance.)

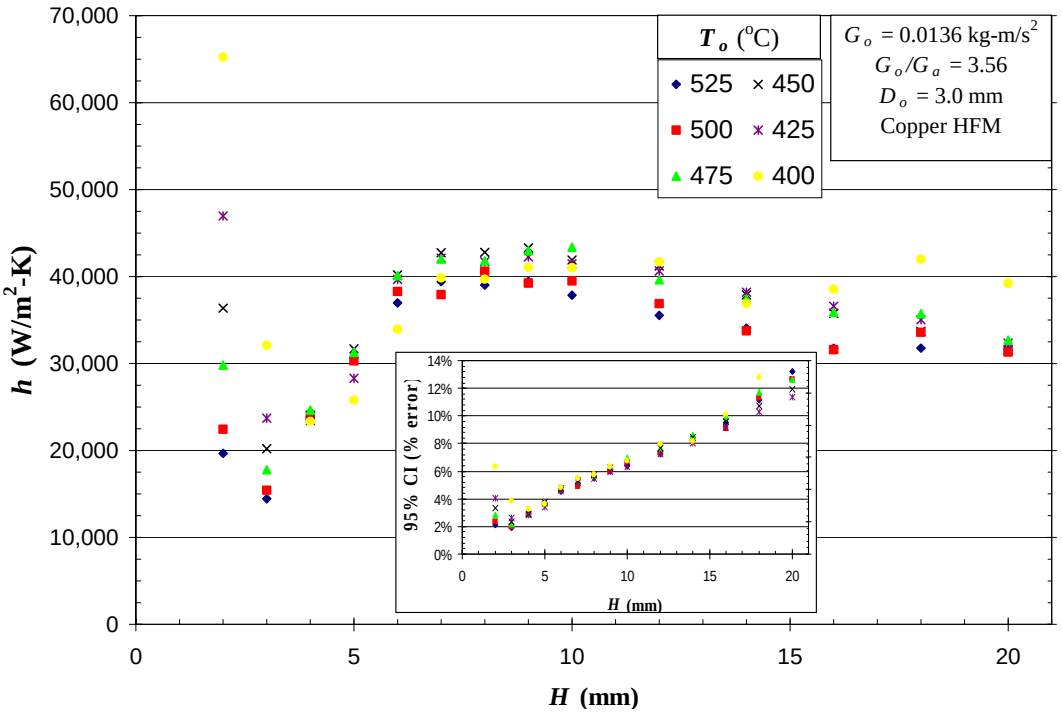

Figure 10. Measured heat flux for jets impinging against a flat surface as a function of stand-off distance for a range of nozzle exit temperatures and jet momentum flux of G_o = 0.0136 kg-m/s^2. (Inset: 95%CI of error measurement as a function of nozzle exit temperature and stand-off distance.)

Compared to previous spallation experiments, the heat fluxes measured using the brass and copper HFM's for the jets in this study should be more than adequate to induce thermal spallation in rocks, even for large stand-off distances. However, the free jet temperature measurements in Section 5 and the stagnation temperature measurements here show that very small stand-off distances are required to be able to heat the rock surface to a sufficiently high temperature to induce thermal spallation. Using a conservative value of h = ~20,000 W/m^2-K for the heat transfer coefficient of an impinging supercritical jet, a temperature difference of 50 ^{o}C between the jet and rock surface would deliver a heat flux of 1 MW/m^2 to the rock surface. Based on these results and the observations of previous researchers in our group, a jet with a nozzle exit temperature of 525 ^{o}C should be able to induce thermal spallation in the rock surface at a stand-off distance of 1-2 nozzle diameters. The results of these studies indicate that thermal spallation is feasible in a high pressure, high density, aqueous environment similar to that which could be encountered in deep borehole conditions. They also support the conclusion that the reason spallation was not observed in the experiments on rock samples was due to insufficient rock sample size and not because of insufficient temperatures or heat fluxes.

7. Conclusions

An autoclave reaction system was designed and constructed to create flame jets in water at a pressure of 250 bar. Experiments using methanol and hydrogen as fuels demonstrated that hydrothermal flames can be produced in a downhole environment. Flame temperatures in excess of 1000 ^{o}C were measured. Attempts were made to use the

flames to spall small rock samples. A flame spallation test on Sioux quartzite showed that spallation occurred initially, but then stopped. It was inferred from thermally induced cracks that ran the length of the sample that the entire surface had been heated, causing spallation to stop due to a lack of confining stresses. It was concluded that the maximum rock sample size that could be used in the WCHB was too small for continuous spallation to be maintained.

The experimental system was modified to study the centerline temperature decay of non-isothermal turbulent free jets of water at supercritical temperatures injected into subcritical temperature water. Jet nozzle exit temperatures ranging from 300 to 525 ^{o}C, corresponding to initial density ratios ranging from 1.35 to 12.1, were studied. The jet was divided into two regions: the far-field region and the jet development region. In the far-field, where the density gradient between the jet and ambient fluid was small, the axial temperature decay followed conventional jet scaling laws, indicating that the jet flow was self-similar. The Thring-Newby scaling law accurately accounted for the large initial density ratio between the nozzle exit and ambient fluid. However, the slope of the axial decay of the jets varied slightly as a function of the initial density ratio. The variation was attributed to experimental conditions rather than being a characteristic of the axial temperature decay of supercritical jets. In the jet development region, supercritical jets were observed to be quickly quenched to below the critical temperature of water within one or two diameters of the nozzle exit due to rapid entrainment of ambient fluid.

A device for measuring heat flux in the experimental system was designed, constructed, and used to determine the heat transfer coefficients of sub- and supercritical temperature jets impinging against a flat surface. A two-dimensional model of heat conduction in the heat flux meter (HFM) was used to optimize its design. Maximum heat fluxes of 1.7 MW/m^2 and 4.6 MW/m^2 were measured using HFM's constructed out of brass and copper, respectively. Heat transfer coefficients ranging from 30,000 to 40,000 W/m^2-K were calculated for stand-off distances in the far-field region for jets with both sub- and supercritical nozzle exit temperatures. For supercritical temperature jets, the heat transfer coefficient dropped significantly to values of less than 20,000 W/m^2-K in the area of the jet development region where the stagnation temperature transitions from subcritical to supercritical values.

The studies of the axial temperature decay and heat flux from impinging supercritical temperature jets indicate that the necessary temperatures and heat fluxes required to induce thermal spallation in rocks can be achieved in a deep borehole. However, small stand-off distances of one or two nozzle diameters are required to be able to heat the rock surface to a sufficiently high temperature to induce thermal spallation under the experimental conditions studied.